Available online at www.sciencedirect.com
ScienceDirect
Icarus 187 (2007) 442–456
ICARUS
www.elsevier.com/locate/icarus

Assessing the limits of the Modified Gaussian Model for remote spectroscopic studies of pyroxenes on Mars

Lisa C. Kanner *, John F. Mustard, Aline Gendrin

Department of Geological Sciences, Brown University, 324 Brook Street, Box 1846, Providence, RI 02912, USA

Received 24 May 2006; revised 25 September 2006

Available online 15 December 2006

Abstract

We investigate the ability to refine pyroxene composition and modal abundance from laboratory and remotely acquired spectra. Laboratory data including the martian meteorites, Shergotty, Zagami, MIL03346, and ALH84001 as well as additional pyroxene-rich spectra obtained from the OMEGA (Observatoire pour la Minéralogie, l'Eau, les Glaces, et l'Activité) spectrometer for Mars are characterized using the Modified Gaussian Model (MGM), a spectral deconvolution method developed by Sunshine et al. [Sunshine, J.M., Pieters, C.M., Pratt, S., 1990. J. Geophys. Res. 95, 6955–6966]. We develop two sensitivity tests to assess the extent to which the MGM can consistently predict (1) pyroxene composition and (2) modal abundance for a compositionally diverse suite of pyroxene spectra. Results of the sensitivity tests indicate that the MGM can be appropriately applied to remote spectroscopic measurements of extraterrestrial surfaces and can estimate pyroxene composition and relative abundance within a derived uncertainty. Deconvolved band positions for laboratory spectra of the meteorites Shergotty and Zagami are determined within ±17 nm while remotely acquired OMEGA spectra are defined within ±50 nm. These results suggest that absolute compositions can be uniquely derived from laboratory pyroxene-rich spectra and non-uniquely derived from the remote measurements of OMEGA at this time. While relative pyroxene chemistries are not assessed from OMEGA measurements at this time, relative pyroxene abundances are estimated using a normalized band strength ratio between the low-calcium (LCP) and high-calcium (HCP) endmember components and are constrained to ±10%. The fraction of LCP in a two-pyroxene mixture is the derived value from the normalized band strength ratio, LCP/(LCP + HCP). This calculation for relative abundance is robust in the presence of up to 10–15% olivine. Deconvolution results from the OMEGA spectra indicate that the ancient terrain in the Syrtis Major region is uniquely enriched in LCP (59 ± 10% LCP) relative to HCP while the volcanics of Syrtis Major are uniquely enriched in HCP (39 ± 10% LCP).

Keywords: Infrared observations; Mars, surface; Mineralogy; Spectroscopy

1. Introduction

The determination of martian crustal compositions is essential to understanding the evolution of the surface as well as the mantle. Analyses of hand samples and remote spectroscopic measurements offer important insights into crustal compositions. The SNC (Shergottites, Nakhlites, and Chassignites) meteorites, which are assumed to have originated from Mars, are depleted in Al_2O_3 and CaO relative to terrestrial basalts (Longhi et al., 1992) and exhibit a mineralogy dominated by pyroxene and plagioclase with various amounts of olivine and Fe–Ti oxides (McSween, 1994). However, it is difficult to assess how well they characterize the surface because the exact source regions of the SNC samples are still unknown.

The global, high-resolution coverage from remotely acquired spectroscopic measurements provides the geologic context necessary for the interpretation of SNC meteorites. Near-infrared and thermal spectroscopic analyses indicate the presence of large fractions of low-calcium and high-calcium pyroxene across the martian surface as well as localized concentrations of olivine (Bandfield, 2002; Bibring et al., 2005; Mustard et al., 2005). The strongest signals of low-calcium pyroxene are focused in the ancient cratered terrain while the Hesperian volcanics of Syrtis Major and mobile materials, such as wind streaks and sand dunes, reveal an enrichment of high-calcium pyroxene (Mustard et al., 2005). The two-pyroxene

* Corresponding author. Fax: +1 401 863 3978.
E-mail address: lisa_kanner@brown.edu (L.C. Kanner).

0019-1035/$ – see front matter
doi:10.1016/j.icarus.2006.10.025

compositions described by these measurements are typical of all basaltic SNC meteorites except for the pure orthopyroxenite, which is also the oldest (∼4.5 Ga) (Mittlefehldt, 1994; Mustard and Sunshine, 1995). These remotely acquired datasets can be used directly to search for SNC lithologies and source regions for the martian meteorites (Hamilton et al., 2003).

The character of pyroxene composition and distribution on the martian surface has significant implications on mantle evolution. Substantial fractions of low-calcium pyroxene may be indicative of a source depleted in calcium and/or larger degrees of partial melt. Only terrestrial komatiites, which are produced by 30% melting, and lunar mare basalts, exhibit uniquely low concentrations of aluminum and calcium similar to the SNC meteorites (Hess and Parmentier, 2001). Furthermore, mantle evolution on Mars may be similar to the Moon and explained by magma ocean processes and a density driven overturn to form a compositionally stratified mantle (Hess and Parmentier, 2001; Elkins-Tanton et al., 2003).

In this paper, we aim to constrain estimates for pyroxene compositions and modal abundances from visible-near infrared (VNIR) reflectance spectra to better characterize the evolution of planetary surfaces. For such pyroxene characterization, we utilize the Modified Gaussian Model (MGM) developed by Sunshine et al. (1990), which deconvolves spectra into its individual absorption components. Studies have been conducted to test the ability of the MGM to predict modal abundance (e.g., Sunshine and Pieters, 1993) and subsequent analysis have attempted to correlate deconvolved band positions to pyroxene composition (e.g., Sunshine et al., 1993; Mustard and Sunshine, 1995; Mustard et al., 1997; Schade et al., 2004). Here, we explicitly address the ability of the MGM to repeatedly predict unique composition and modal abundance for a variety of laboratory and remotely acquired pyroxene-rich spectra. We develop two sensitivity tests: the first examines composition and the second investigates modal abundance. The results of these tests are assessed to determine uncertainties that can then be applied to MGM derived estimates on composition and modal abundance. While all extra-terrestrial samples used in this analysis include spectra of the surface of Mars, the application of the MGM and derived uncertainties can be used with MGM derived solutions of pyroxene-rich spectra for many of the rocky bodies in the inner Solar System.

2. Background

2.1. Pyroxene spectroscopy

Pyroxene reflectance spectra are characterized at VNIR wavelengths by two strong absorption features with minima near 1 and 2 μm and a weaker feature at 1.2 μm. All three absorptions are the result of crystal field transitions of iron in octahedral coordination. The absorption at 1.2 μm is the result of molecular distortion in the M1 crystallographic site while the dominant 1- and 2-μm absorptions are attributed to the M2 site (Burns, 1993). While an additional M1 absorption is also predicted at 0.9 μm, it is usually obscured by the stronger M2 absorption at the same location (Burns, 1993). The characteristic shape of the absorption features is a function of site symmetry and bond length. Thus, the substitution of different sized cations, such as calcium, iron, and magnesium, has significant effects on the position and shape of each feature (Adams, 1974; Cloutis and Gaffey, 1991). For this study, we are interested in calcium and iron substitutions, which are known to have the most significant effects on the band position by systematically shifting the 1- and 2-μm features to longer wavelengths with increasing abundance (Adams, 1974; Cloutis and Gaffey, 1991; Klima et al., 2005). For example, the band centers of low-calcium pyroxenes (e.g., orthopyroxenes and low-calcium clinopyroxenes) occur near 0.9 and 1.8 μm while the band centers of high-calcium pyroxenes (e.g., calcic-clinopyroxenes) are located near 1.05 and 2.3 μm (Adams, 1974; Cloutis and Gaffey, 1991). For sufficiently high M1 ferrous iron site occupancy, the M2 and M1 absorptions at ∼1 μm can be observed for calcic-clinopyroxenes (Cloutis, 2002; Schade et al., 2004). Because of these characteristic differences between low-calcium and high-calcium pyroxenes, absorption band position can be used for compositional estimates. However, in the presence of pyroxene mixtures it is difficult to reliably isolate the endmember components. The Modified Gaussian Model (MGM) developed by Sunshine et al. (1990) has the potential to resolve these endmember fractions.

2.2. Modified Gaussian Model (MGM)

It is possible to estimate pyroxene compositions and relative abundances from near-infrared spectra using the MGM (Sunshine et al., 1990). This method deconvolves overlapping absorptions of mafic mineral spectra into their fundamental absorption components. Individual absorption components are modeled as modified Gaussian distributions that mathematically describe the specific shape of electronic transition absorptions and are parameterized by a band center, band width, and band strength. Spectra are modeled as a sum of modified Gaussian distributions superimposed on a baseline continuum that is defined by a slope and an offset and can be linear in wavelength or in wavenumber (Fig. 1). MGM computations are carried out in energy and natural log reflectance space and thus overlapping absorptions are additive and can be modeled using linear inverse theory (Sunshine et al., 1990). The inversion method applied in Sunshine et al. (1990) is the stochastic inversion of Tarantola and Valette (1982) that allows for the inclusion of a priori information as constraints on the solutions. These constraints include general model starting uncertainties on all parameters that together govern the magnitude of change during the inversion. Sunshine and Pieters (1993) showed that the constraints helped to stabilize the inversion process and prevent physically unrealistic solutions. The inversion is an iterative process and all absorption band parameters and the continuum are free to move until the residual errors, which are calculated as the difference between the log of the actual spectrum and the log of the modeled spectrum, are minimized (Sunshine et al., 1990).

The Modified Gaussian Model has been shown to successfully model overlapping absorptions in several previous studies

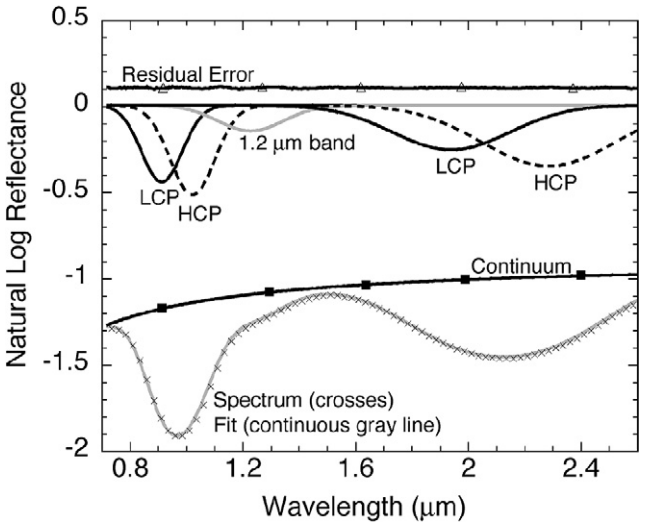

Fig. 1. Sample MGM fit for the martian meteorite, Zagami. The MGM deconvolves spectra into its individual absorption components, by fitting a series of modified Gaussian distributions (solid black and dashed lines) superimposed on a baseline continuum (solid black line with squares). Two absorptions, representing the low-calcium (LCP) absorptions (solid black line) and high-calcium (HCP) absorptions (dashed line), are needed to appropriately describe the dominant 1- and 2-μm absorption features. An additional absorption is necessary at ∼1.2 μm (labeled solid gray line). The error (solid black line with open triangles) is measured as the difference of the log of the actual spectrum (crosses) and the log of the modeled spectrum (continuous gray line) and is offset by +0.1 log reflectance for clarity.

(e.g., Sunshine and Pieters, 1993; Mustard and Sunshine, 1995; Schade and Wäsch, 1999; Hiroi and Sasaki, 2001; Schade et al., 2004; Sunshine et al., 2004a, 2004b). The appropriate number of deconvolved absorptions is dependant on the of number of endmembers present in the material measured and the number of unique crystal field absorptions for each endmember. Sunshine et al. (1990) demonstrated that for a spectrum of pure enstatite, a low-calcium pyroxene, the major absorption features at 1 and 2 μm are appropriately fit with single modified Gaussian distributions. Similarly, for a spectrum of pure diopside, the high-calcium endmember, only one absorption is required for each of the 1- and 2-μm features. Thus, enstatite and diopside mixtures are described by two absorptions at both 1 and 2 μm that correspond to the low-calcium (LCP) and high-calcium (HCP) endmember components (Sunshine et al., 1990; Sunshine and Pieters, 1993). Typically the 1.2-μm feature is modeled as one absorption when fitting endmember or mixture spectra (Sunshine and Pieters, 1993). For LCP and HCP mixtures of various abundances, the band positions of the major LCP and HCP components remain essentially fixed at the endmember values while the strengths vary as a function of modal abundance (Sunshine et al., 1990; Sunshine and Pieters, 1993). Sunshine and Pieters (1993) explored the effects of particle size on the correlation between relative component band strength and percent HCP for a physically mixed enstatite–diopside suite. A relationship was determined between the fraction of high-calcium pyroxene in the mixture and the band strength ratio, LCP/HCP, in the 1- and 2-μm regions for all particle sizes (Fig. 7 in Sunshine and Pieters, 1993).

The systematic study of the enstatite–diopside mixture series has three important implications for the interpretation of MGM solutions: (1) fits are independent of particle size; (2) no prior knowledge of endmember pyroxene composition is necessary in order to obtain an acceptable fit; and (3) the relationship between %HCP and the LCP/HCP band strength ratio promises to predict the relative abundance of LCP and HCP of an unknown mixture. These implications establish the unique value of the MGM in data analysis of remotely acquired spectra where the particle size, endmember compositions, and relative abundances are unknown. Previous studies have used the MGM on remotely acquired VNIR reflectance spectra to extract relative abundances (e.g., Gendrin et al., 2006) and, to a certain extent, pyroxene compositions (e.g., Mustard and Sunshine, 1995; Mustard et al., 1997) for investigation of the origin and evolution of the martian surface. Using ISM (Imaging Spectrometer for Mars) data, Mustard and Sunshine (1995) was one of the first studies to apply the MGM to remotely acquired spectra.

Refinement of pyroxene compositions and modal abundances provides the potential for major advancements in petrologic studies of the martian surface and other rocky bodies. The MGM promises to estimate composition and modal abundance without prior knowledge of the endmembers. However, the precision and accuracy of MGM band position solutions has not been explicitly investigated for pyroxenes with a broad range of iron content and with data of lower precision than laboratory data. Although formal uncertainties are derived output of the model, they can be difficult to apply. The formal uncertainty on the model results are a function of the quality of the input data as well as the suitability of the model to fit the data. For example, model output uncertainties will increase significantly for low signal-to-noise of the observed data, low spectral contrast of the observed data or for the inclusion of more model parameters (i.e., modified Gaussians) that is warranted by the observations. For remotely acquired data, it is likely that the MGM can derive band position more precisely than suggested by the formal output model uncertainties. An addition cause for more detailed investigation is that estimates of modal abundance are derived from one enstatite–diopside mixture series (Sunshine and Pieters, 1993). Thus, further assessments of MGM strengths and limitations are important for confident use of the model for extraterrestrial surfaces.

For this study, we evaluate the performance of the MGM under a variety of conditions and attempt to provide revised uncertainty parameters with which to interpret final MGM results for remotely acquired pyroxene-rich spectra. We design two sensitivity tests to be incorporated in our interpretations. In the first test, we develop an uncertainty parameter on band position that is complementary to the formal output uncertainties. We systematically vary the starting band position parameters and assess the consistency of resultant band solutions. For the second investigation, we vary the endmember composition by incorporating iron-rich pyroxene mixtures and assess the relationship between relative band strength and modal abundance. We apply the results of these tests to MGM solutions of OMEGA pyroxene-rich spectra.

3. Data

This study incorporates laboratory data of terrestrial and martian meteorite pyroxenes as well as remotely acquired data of the martian surface. All laboratory data were obtained from the Reflectance Experiment Laboratory (RELAB) database at Brown University where measurements were taken using a bidirectional near-infrared spectrometer $i = 30°$ and $e = 0°$ (Pieters, 1983; Pieters and Hiroi, 2004; http://www.planetary.brown.edu/relabdocs/relab.htm). Remotely sensed data were acquired from the imaging near-infrared spectrometer OMEGA (Observatoire pour la Minéralogie, l'Eau, les Glaces, et l'Activité) on the Mars Express satellite. OMEGA operates with a 1.2-mrad IFOV and uses three spectrometers for a total of 352 spectral channels between 0.35 and 5.09 μm (Bibring et al., 2004). The Visible Near-InfraRed (VNIR) detector has a spectral resolution of 7.5 nm between 0.35 and 1.05 μm, the Short Wavelength InfraRed (SWIR) detector a resolution of 14 nm between 0.94 and 2.70 μm and Long Wavelength InfraRed (LWIR) detector a resolution of 21 nm between 2.65 and 5.2 μm (Bibring et al., 2004). Due to an elliptical orbit, the spatial resolution varies from 300 m/pixel at pericenter to 4.8 km/pixel at an altitude of 4000 km. A simple photometric correction is applied to each spectrum by dividing by the cosine of the incidence angle of the observation. An atmospheric correction is performed assuming that the atmospheric and surface contributions are multiplicative and that the atmospheric contribution follows a power law variation with altitude (Bibring et al., 1989). With this assumption, the ratio of a spectrum from the base of Olympus Mons to one over the summit provides a power function of their difference in altitude. Each spectrum is corrected by dividing the observation by the derived atmospheric spectrum scaled by the strength of the CO_2 absorption measured in the observation. Spectra are also spatially and spectrally aligned to account for the discrepancies in overlap between the VNIR and SWIR detectors. The incorporation of both detectors is required to achieve a continuous spectrum between 0.7 and 2.6 μm and thus to apply the MGM across the full expression of the pyroxene crystal field absorptions.

Laboratory spectra used in the band center variation analysis include two whole rock spectra of the shergottite meteorites, Zagami and Shergotty (Fig. 2). These meteorites have been shown to be spectrally and compositionally similar to derived spectra from Mars (Mustard and Sunshine, 1995).

Laboratory spectra used in mixture analyses are plotted in Fig. 3 and the corresponding compositions are shown in Fig. 4 and Table 1.

Samples include six low-calcium pyroxenes (Cloutis and Gaffey, 1991; Sunshine and Pieters, 1993; Bishop et al., 1998; Klima et al., 2005) and four high-calcium pyroxenes (Cloutis and Gaffey, 1991; Sunshine and Pieters, 1993; Dyar et al., 2005).

Two of the pyroxenes are identical to the enstatite–diopside endmembers described in Sunshine and Pieters (1993). Additional low-calcium pyroxenes include a second terrestrial enstatite, a bronzite, two synthetic calcium-free pyroxenes, and a whole rock sample of the martian meteorite ALH84001, an

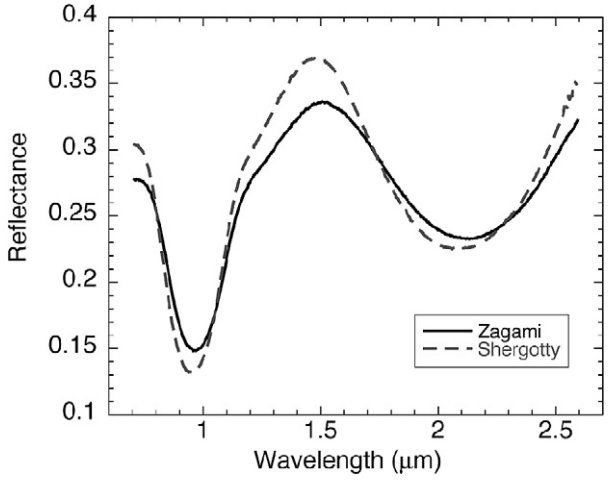

Fig. 2. Martian meteorite spectra, Zagami (solid black line) and Shergotty (dashed gray line), used in the band center variation analysis.

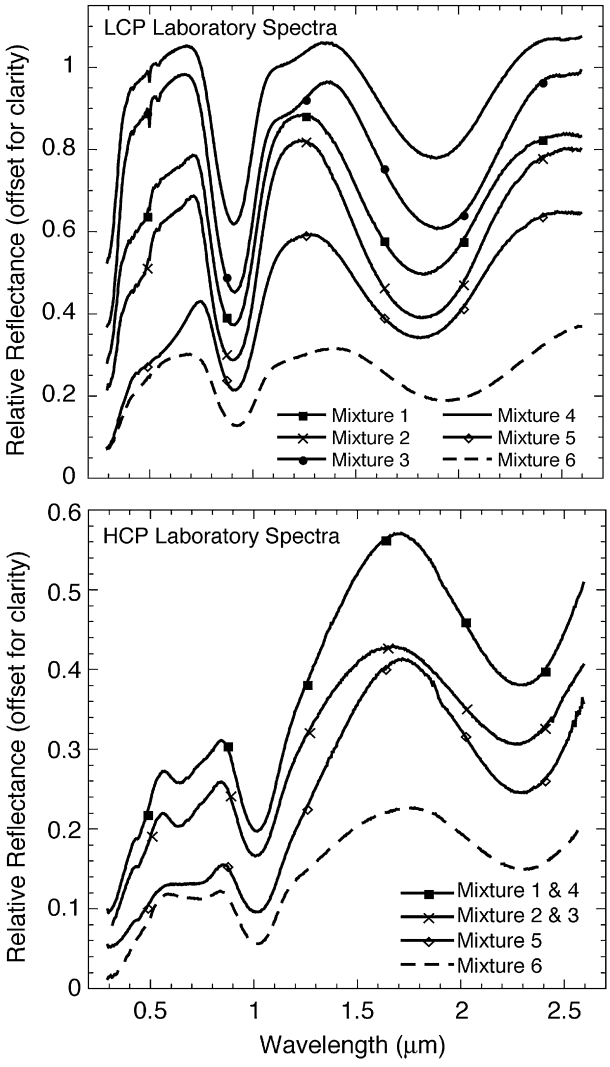

Fig. 3. Low-calcium and high-calcium pyroxene spectra selected from the RELAB database and used in the mixture series analysis. RELAB file identification numbers associated with each mixture are given in Table 1.

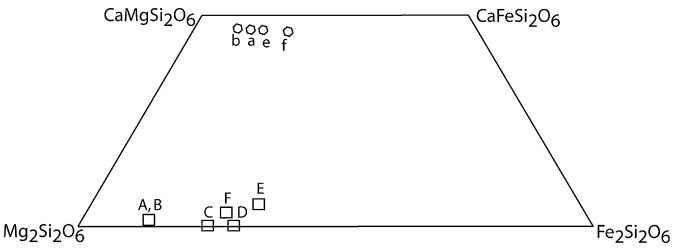

Fig. 4. Compositions of pyroxenes used in the mixture series analysis projected onto the pyroxene quadrilateral. Corresponding RELAB identification numbers are given in Table 1.

Table 1
Low-calcium and high-calcium pyroxene endmembers used in the mixture series analysis

Mixture[a] number		Pyroxene endmember (RELAB File ID)	Particle size (μm)	Wo	En	Fs
Mixture 1	A	C2PE31[b]	45–75	1.5	85.6	12.9
	a	C3PP22[b]	45–75	45.9	43.6	10.5
Mixture 2	B	CBPE34[c]	25–45	1.5	85.6	12.9
	b	C1PP09[c]	45–90	46.2	45.8	8.0
Mixture 3	C	opx22A[d]	0–45	0	75.0	25.0
	b	C1PP09[c]	45–90	46.2	45.8	8.0
Mixture 4	D	opx26A[d]	0–45	0	70.0	30.0
	a	C3PP22[b]	45–75	45.9	43.6	10.5
Mixture 5	E	C1PP40[c]	0–45	5.5	62.1	32.4
	e	C1SC35[c]	45–90	45.7	41.1	13.2
Mixture 6	F	C3MT02[e,f]	0–125	3.3	69.4	27.3
	f	C1DD56[g,h]	0–45	44.5	34.8	20.8

[a] Endmembers are mixed in the following proportions: 85:15, 75:25. 60:40, 50:50, 40:60, 25:75, 15:85 (LCP:HCP).
[b] Sunshine and Pieters (1993).
[c] Cloutis and Gaffey (1991).
[d] Klima et al. (2005).
[e] Bishop et al. (1998).
[f] ALH84001.
[g] Dyar et al. (2005).
[h] MIL03346.

orthopyroxenite. ALH84001 contains approximately 97% low-calcium pyroxene and thus we assume that the shape of the whole rock spectrum is nearly identical to the spectrum of the orthopyroxene separate. Additional high-calcium pyroxenes include a second terrestrial diopside, an augite, and a whole rock sample of the nakhlite martian meteorite MIL03346. Although MIL03346 contains ∼70% high-calcium pyroxene and 3% olivine, the spectrum of the whole rock was shown to be almost identical to the spectrum of the clinopyroxene separate (Dyar et al., 2005).

All OMEGA spectra were selected from the current publicly released dataset, which includes all observations through ORB1100. Averaged spectra used in the band center variation analysis represent samples of LCP-rich and HCP-rich terrains in the Syrtis Major province (Fig. 5). An LCP-rich spectrum was selected from observation ORB0232_2, which covers the contact where younger Hesperian volcanics extend into the ancient LCP-rich cratered terrain (Mustard et al., 2005). Observation ORB0488_3 surveys a large extent of the HCP-rich Syrtis volcanics and a type HCP spectrum was selected from this observation.

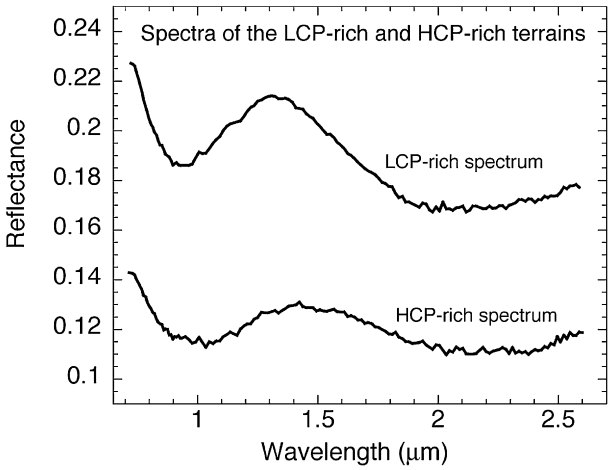

Fig. 5. Averaged OMEGA spectra used in the band center variation analysis. Spectra were selected from an LCP-rich region (observation ORB0232_2) in the ancient cratered terrain north of Syrtis Major and an HCP-rich region (observation ORB0488_3) within the Syrtis Major volcanics.

Additional examples of spatially averaged OMEGA pyroxene-rich spectra were also selected from various regions associated with Syrtis Major and Valles Marineris (Fig. 6), as previously identified in Mustard et al. (2005).

The specific image cube identification numbers and location of averaged pixels for each of the pyroxene-rich terrains selected are described in Table 2 and Fig. 7.

4. Methods

We apply the Modified Gaussian Model to pyroxene-dominated laboratory and remotely acquired spectra (Sunshine et al., 1999; available at http://www.planetary.brown.edu). To include the full expression of crystal field absorptions at 1 and 2 μm, the MGM is applied to the 0.7- to 2.6-μm wavelength region. We follow the method of Sunshine et al. (1990) and assume that the dominant crystal field absorptions are described by modified Gaussian distributions superimposed on a baseline continuum. Our fit uses the same nonlinear least squares inversion as Sunshine et al. (1990) and is described in Tarantola and Valette (1982). All MGM fits are conducted with all parameters free.

4.1. Band center variation

To resolve pyroxene composition from MGM results, it is essential to understand the precision to which deconvolved absorption band minima can be determined, beyond the formal model constraints that can be ambiguous. We develop a measure of this precision by systematically varying the input band center parameters of the modified Gaussians absorptions that describe the LCP and HCP components in the 1- and 2-μm region, we assess the errors as the spread in resulting band positions and compare them to the formal output constraints for OMEGA spectra. We use a Monte Carlo approach, by systematically varying starting band positions, to calculate an uncertainty rather than rely on the formal model output constraints. Our test is applied to the whole rock laboratory spec-

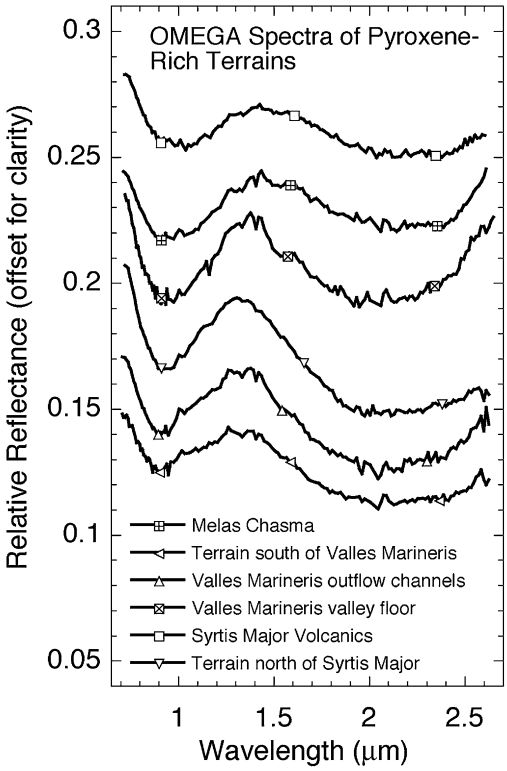

Fig. 6. Averaged OMEGA pyroxene-rich spectra selected from various geologic locations. Observation number and geographic coordinates are given in Table 2.

tra of the martian meteorites Shergotty and Zagami as well as the averaged OMEGA spectra representative of the LCP-rich (ORB0232_2) and HCP-rich (ORB0488_3) terrains.

Each MGM fit for this analysis incorporates six absorptions. Four absorptions correspond to the LCP and HCP endmember components in the 1- and 2-μm regions and additional absorptions are centered near 1.2 μm and either 0.77 μm (SNC meteorite spectra) or 0.85 μm (OMEGA spectra). The difference in the band position of this shortest wavelength absorption is due to the presence of ferric iron on the surface of Mars and thus it is only applied to the OMEGA spectra. The specific values for the input parameters and corresponding constraints are given in Table 3 and are adapted from the values described in Mustard et al. (1997) who applied the MGM to ISM (Imaging Spectrometer for Mars) spectra.

Table 2
Geographic location and orbit number for the averaged OMEGA pyroxene-rich spectra selected from the Syrtis Major (SM) and Valles Marineris (VM) provinces

Geographic location	Orbit number	Lat. °N: Long. °E
SM Hesperian volcanics	0488_3	4.4:66.3
Melas Chasma	0548_2	−13.3:−70.3
VM valley floor	0482_2	−12.0:−64.5
Noachian terrain north of SM	0232_2	21.6:73.3
VM outflow channels	0544_2	−11.7:−38.3
South of VM outflow channels	0511_1	−20.25:−35.3

The starting band positions and widths are identical for the meteorite and OMEGA spectra and vary in the strengths to account for inherent differences in absorption strength between laboratory and remotely acquired spectra. The initial formal constraints on the band positions used in this study are slightly weaker than those of Mustard et al. (1997) to ensure that the constraints are larger than the spread of band positions applied in our Monte Carlo variation. We use a nonlinear continuum in wavelength space (linear in wavenumber) for the laboratory meteorite spectra, which is consistent with Sunshine et al. (1993, 2004a) who also applied the MGM to laboratory martian meteorite spectra. We incorporate a lin-

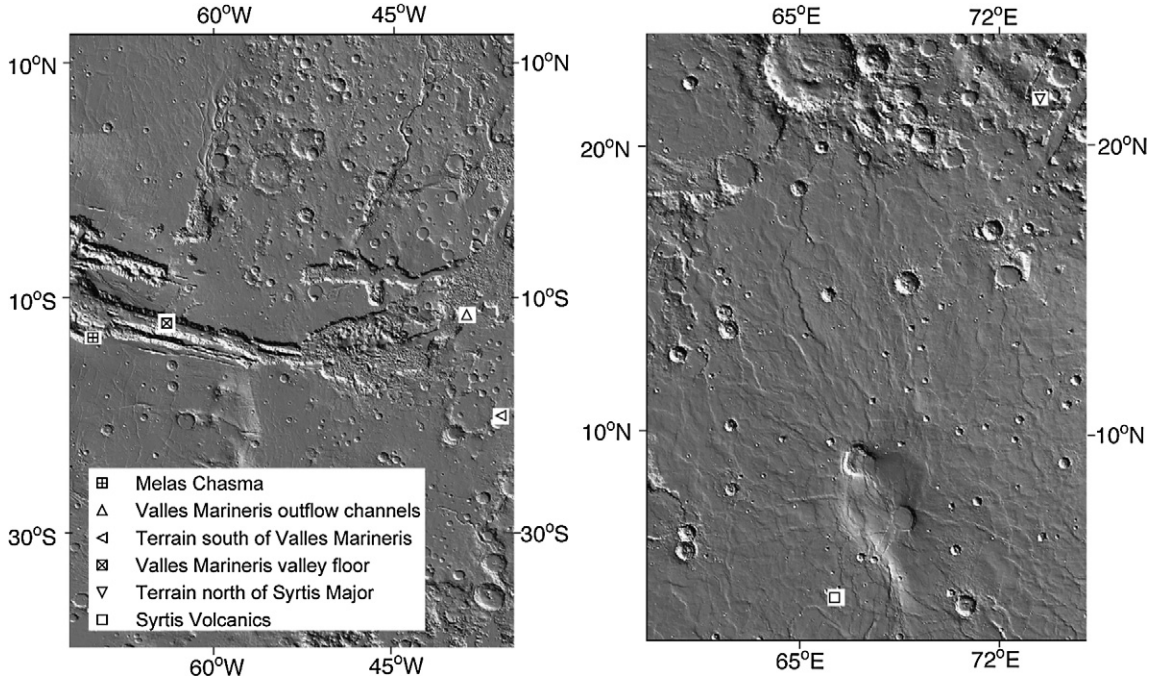

Fig. 7. Map of the averaged OMEGA pyroxene-rich spectra selected from the Valles Marineris (left) and the Syrtis Major (right) provinces.

Table 3
Initial MGM absorption parameters for the Zagami, Shergotty, and OMEGA LCP-rich and HCP-rich spectra used in the band center sensitivity test

Spectral feature	Band center (μm)	Band width (μm)	Band strength (natural log reflectance)	
			Meteorite	OMEGA
Electronic transition	0.770 0.100	0.157 0.200	0.100 1.5	
Ferric band	0.850 0.100	0.200 0.200		0.040 1.0
LCP 1 μm	0.901 0.200	0.189 0.200	0.300 1.5	0.060 1.5
HCP 1 μm	1.025 0.200	0.187 0.200	0.300 1.5	0.060 1.5
1.2-μm band	1.155 0.200	0.250 0.200	0.100 1.5	0.040 1.5
LCP 2 μm	1.900 0.300	0.500 0.200	0.300 1.5	0.060 1.5
HCP 2 μm	2.300 0.300	0.560 0.200	0.300 1.5	0.060 1.5

ear continuum in wavelength space for all fits to OMEGA data.

The same range of starting band positions is used for each laboratory and OMEGA spectrum and is representative of the range in band minima for single-phase terrestrial pyroxenes (Cloutis and Gaffey, 1991). For each spectrum, there are a total of 45 model runs. At 25 nm increments, we vary the input band centers in the 1-μm region from 0.875 to 0.95 μm for the LCP component and from 0.975 to 1.075 μm for the HCP component. At 50 nm increments, we vary the input parameters in the 2-μm region from 1.8 to 2.0 μm and from 2.2 to 2.4 μm, for the LCP and HCP components, respectively. While the initial band centers were spaced at fixed increments, they were allowed to vary to iteratively converge to a fit.

MGM results are evaluated under four criteria. A final solution was considered inappropriate and not included in the resultant analyses if (1) the RMS residual error was greater than 2×10^{-4}, (2) the change in the RMS error from the previous fit was greater than 10^{-5}, (3) the difference in the LCP/(LCP + HCP) band strength ratios in the 1 and 2 μm was greater than 10^{-1}, or (4) the continuum intersected the applied spectrum. The RMS error criteria are consistent with those used in the model developed by Sunshine et al. (1990). Criterion (3) is applied because the relative band strengths of the LCP and HCP absorptions should be similar in the 1- and 2-μm regions and the normalized band strength ratio can be used to examine relative changes in the modal abundance (Sunshine and Pieters, 1993).

In the band center sensitivity test, forty-nine percent of the model runs for the Zagami meteorite and forty-four percent for the Shergotty meteorite met the described criteria. For the OMEGA spectra, forty-four percent were successful for the LCP-rich terrain and twenty-seven percent for the HCP-rich terrain. The majority of unsuccessful fits occurred for the maximum and minimum starting values.

4.2. Endmember mixing

The endmember mixing analysis was designed to assess the LCP/HCP band strength ratio for pyroxene mixtures of a variety of compositions. This ratio was initially calculated from an enstatite–diopside pair of relatively low iron content (Sunshine and Pieters, 1993). Because only one enstatite–diopside suite was used in all subsequent applications of modal abundance, and because pyroxenes on extraterrestrial bodies have comparatively higher iron contents, it is important to test the performance of the MGM for mixtures of various pyroxene compositions. Sunshine et al. (1993) have previously noted the importance of applying the MGM to a compositional suite of pyroxenes. The RELAB dataset was thoroughly examined to extract the widest compositional range of uncontaminated single-phase pyroxene spectra. Eight qualified pyroxene spectra, three high-calcium and five low-calcium, were identified in addition to the enstatite and diopside endmembers of Sunshine and Pieters (1993). Six mixture series were constructed each with a low-calcium and high-calcium endmember. Endmembers with similar modal iron contents were paired, which is the expectation of naturally coexisting pyroxene phases (Cameron and Papike, 1980).

Each pyroxene mixture series was calculated directly from the endmember spectra. This mixing procedure is identical to that of Mustard and Pieters (1987) who examined the validity of calculating mixtures of equivalent particle size. In this analysis, we assume an intimate (nonlinear) mixing regime, where the path length of the photon is larger than the particle size of the components in the mixture. We incorporate the nonlinear photometric mixing model of Hapke (1981, 1986) to create a lookup table and convert reflectance values to single scattering albedo. We use the assumptions from Mustard and Pieters (1987) who showed it reasonable to assume that the backscatter function is negligible and that the phase function for an isotropic system is equal to 1.0 when the phase angle, as in our measurements, is 30°. When nonlinear behavior of intimate mixtures is predicted in reflectance space, linear behavior is predicted in single scattering albedo space (Hapke 1981, 1986). Thus, the LCP and HCP endmembers were linearly mixed in single scattering albedo space in the following proportions, 85:15, 75:25, 60:40, 50:50, 40:60, 25:75, and 15:85, which are identical to those used in the Sunshine and Pieters (1993) particle size analysis. Final mixture spectra were converted back into reflectance for MGM application.

To evaluate our endmember mixing calculations, we compared our calculated enstatite–diopside mixture series with the physically mixed series of identical endmembers from Sunshine and Pieters (1993). Both the physical and the calculated mixtures gave equivalent results in reflectance space. The calculated mixture series also is modeled with identical MGM parameters as the physical mixture from Sunshine and Pieters (1993). The congruence in spectral shape and MGM parameters between the calculated and physically mixed mixtures validates the calculated mixing methodology for all endmembers in this analysis.

Table 4
Initial MGM parameters and constraints used in the mixture series analysis

	Spectral feature	Band center (μm)	Band width (μm)	Band strength (natural log reflectance)
Band 1	Electronic transition	0.744 0.100	0.157 0.200	0.090 1.500
Band 2	LCP 1 μm	0.911 0.100	0.214 0.200	0.300 1.500
Band 3	HCP 1 μm	1.012 0.100	0.215 0.200	0.300 1.500
Band 4	1.2-μm band	1.159 0.100	0.303 0.200	0.100 1.500
Band 5	LCP 2 μm	1.854 0.300	0.602 0.300	0.300 1.500
Band 6	HCP 2 μm	2.290 0.300	0.559 0.300	0.300 1.500
Band 7		2.520 0.100	0.511 0.200	0.010 1.500

The MGM was applied to all endmember and calculated mixture spectra. Seven individual absorptions were used, four of which describe the LCP and HCP endmembers at 1 and 2 μm, and three others are centered at 0.744, 1.159, and 2.52 μm (Sunshine and Pieters, 1993). The number of absorptions and starting conditions were adapted from the parameters of Sunshine and Pieters (1993) for terrestrial pyroxenes and are described in Table 4. We use a nonlinear continuum in wavelength space. These starting conditions vary slightly from those used in the first sensitivity test of the martian spectra in that they are adapted for the terrestrial pyroxene mixture (Mixture #1) from Sunshine and Pieters (1993). Aside from the continuum, which is varied slightly for each mixture series to account for differences in albedo and slope, the starting conditions for the band centers, widths, and strengths were identical for all endmember and mixture spectra. A total of fifty-four MGM fits were evaluated: seven mixture spectra and two endmembers for each of six sets of endmembers.

The validity of final MGM fits was determined in an identical manner to the results of band center sensitivity tests. The aforementioned criteria exclude fits above a defined error threshold, those with inconsistent 1- and 2-μm component band strengths, and those where the continuum intersects with the input spectrum. In this mixture series analysis, 76% of the solutions met the acceptance criteria.

To assess the validity of the band strength relationship when other minerals are present, we conducted a first-order investigation by systematically adding an olivine spectral component to Mixture #1. The addition of the third component to the mixture is justified in that Mustard and Pieters (1989) showed that abundances estimates from spectral mixing in single scattering albedo space is accurate to within 5–10%. In our analysis, we detect changes that are greater than 10%. For spectral mixing, we selected an olivine (RELAB ID# CASC02) whose band depth of 50% is similar to the 45% band depth of the LCP component. Using the same relative proportions of LCP and HCP as previously calculated for Mixture #1, we calculated 5, 10, 15, and 20% of olivine into Mixture #1 using the assumptions of Hapke (1981, 1986). Thus, we obtain four new mixture suites for MGM evaluation. We applied the MGM using identical starting parameters (absorptions and continuum) as the pyroxene only mixture of Mixture #1. In this way, we could determine the maximum fraction of olivine that could be present without affecting the modeled pyroxene results within the calculated uncertainty.

4.3. Application to OMEGA

Using all free parameters and a linear continuum in wavelength space, the MGM was also applied to averaged OMEGA pyroxene-rich spectra (Fig. 6, Table 2) as previously identified in Mustard et al. (2005). While the MGM has previously been applied to OMEGA data using only the 2-μm region (Gendrin et al., 2006), here we incorporate a more complete wavelength regime inclusive of the 1- and 2-μm regions. To test the full capabilities of the model we must extrapolate from the laboratory spectra to remote measurements where spectra are characterized by decreased spectral contrast and increased noise. The MGM solutions to OMEGA data were evaluated using the results from the sensitivity tests of band positions and relative band strength as developed in the previously described investigations.

5. Results

5.1. Sensitivity Test 1: Band center variation

The purpose of the band center sensitivity test is to examine the effect of the input parameters on the final solutions and to determine an uncertainty on resultant band positions for laboratory meteorite data and OMEGA remotely acquired data. We perform this sensitivity test recognizing that the formal MGM output constraints for remotely acquired data may not accurately reflect the true performance of the MGM. The formal uncertainties are typically larger than the separation of bands, yet experience shows that the model consistently achieves better discrimination. The ability to refine pyroxene composition using the MGM requires complete understanding of the extent to which the MGM can find unique band positions.

First-order examination of final band parameters as correlated to the starting band positions reveals that the starting parameters do have a significant effect on the resultant solutions. We observed that as the input band center parameters increase, the resultant solutions similarly shifted to longer wavelengths at ∼25 nm increments. These trends were observed in the 1- and 2-μm regions for the Zagami and Shergotty meteorites as well as for the OMEGA spectra. The ranges of the final acceptable solutions are examined as an average and standard deviation and are described below.

5.1.1. Meteorite spectra

Inclusive of all appropriate fits, the Zagami and Shergotty meteorites returned average band centers in the 1- and 2-μm regions within the range of terrestrial pyroxene band positions (Adams, 1974; Cloutis and Gaffey, 1991; Fig. 8). We note

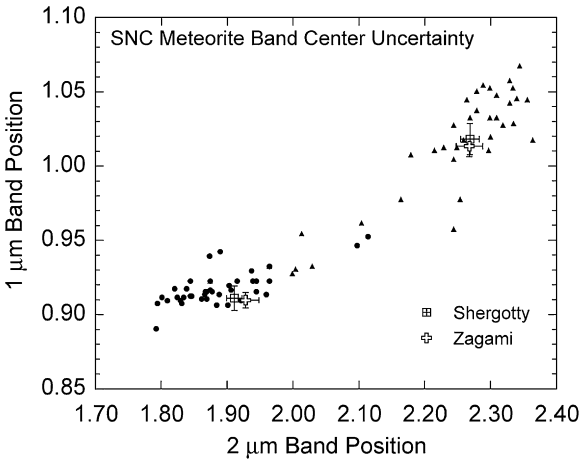

Fig. 8. Averaged MGM derived band positions and uncertainty for the martian meteorites Shergotty (square) and Zagami (cross). Meteorite band positions are plotted with the band positions for single-phase terrestrial pyroxenes as measured by Adams (1974) and Cloutis and Gaffey (1991). Orthopyroxenes are given by closed circles, clinopyroxenes by closed triangles. Averaged uncertainty is ±8 nm and ±17 nm for the 1-μm and 2-μm regions, respectively.

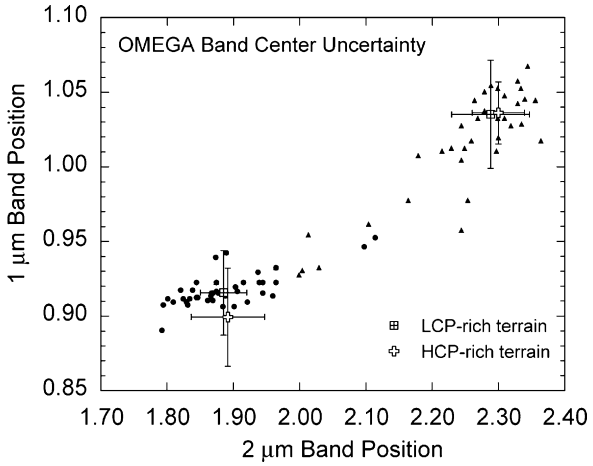

Fig. 9. Averaged MGM derived band positions and uncertainty for LCP-rich (square) and HCP-rich (cross) terrain selected from the Syrtis Major region. OMEGA spectra are plotted with the band positions for single-phase terrestrial pyroxenes as measured by Adams (1974) and Cloutis and Gaffey (1991). Orthopyroxenes are given by closed circles, clinopyroxenes by closed triangles. Averaged uncertainty is ±30 nm and ±47 nm for the 1-μm and 2-μm regions respectively.

that while the terrestrial pyroxene band positions from Adams (1974) and Cloutis and Gaffey (1991) are determined without a continuum removal, the band centers described in this analysis from MGM final solutions are continuum removed. Continuum removed band positions occur on average 7 nm higher than band minima that are not continuum removed (Cloutis and Gaffey, 1991) and thus we make general comparisons between band positions derived in this study those terrestrial pyroxenes tabulated from Adams (1974) and Cloutis and Gaffey (1991).

For both the Zagami and Shergotty meteorites, the LCP components plot clearly in the LCP field and the HCP components plot clearly in the HCP field. Averaged band positions for the LCP and HCP components of the Shergotty and Zagami meteorites are nearly identical (Table 5, Fig. 8).

Zagami band positions of the LCP component in the 2-μm region plot at slightly longer wavelengths compared to Shergotty. Taken at face value this would imply differences in the calcium or iron content of the pyroxenes (Cloutis and Gaffey, 1991). However, our uncertainty calculated by assessing the spread of resultant solutions shows that they are indistinguishable within an average of ±17 nm. The small differences between the means of the band centers for the Zagami and Shergotty meteorite spectra exist within the derived uncertainty of the method.

Based on the pyroxene compositions of Zagami and Shergotty (Stopler and McSween, 1979), the expected band positions for the low-calcium component range from 0.92 to 0.94 and 1.9 to 2.05 μm and for the high-calcium component from 1.0 to 1.02 and 2.2 to 2.3 μm (Cloutis and Gaffey, 1991). The MGM derived band positions in this study (Table 5) are consistent, within the uncertainty, with the expected band positions from known compositions.

5.1.2. *OMEGA spectra*

Band center sensitivity results for the spatially averaged LCP-rich and HCP-rich OMEGA spectra show similar trends to the martian meteorites (Fig. 9). The HCP components plot clearly in the HCP field and the average band positions are nearly indistinguishable.

Small differences are observed between the two terrains with regard to the LCP components. For the LCP-rich terrain, the band positions plot clearly in their corresponding fields. However, the 1-μm LCP component for the HCP-rich terrain occurs at shorter wavelengths compared to the trend for terrestrial pyroxenes. Nevertheless, the small differences in band positions for the OMEGA spectra do not lie outside of the statistical uncertainty of the method. The full range of uncertainty is congruent with the range of values of the terrestrial pyroxenes.

Table 5
Band position and standard deviation derived in the band center sensitivity test

Spectral feature	Zagami meteorite (band center μm)	Shergotty meteorite (band center μm)	LCP-rich terrain (band center μm)	HCP-rich terrain (band center μm)
LCP 1 μm	0.910 ± 0.005	0.911 ± 0.008	0.916 ± 0.028	0.900 ± 0.033
HCP 1 μm	1.014 ± 0.007	1.019 ± 0.010	1.036 ± 0.036	1.037 ± 0.021
LCP 2 μm	1.927 ± 0.020	1.910 ± 0.012	1.884 ± 0.035	1.891 ± 0.055
HCP 2 μm	2.267 ± 0.020	2.268 ± 0.014	2.287 ± 0.059	2.300 ± 0.040

Note. Averaged uncertainty for the meteorite spectra are ±8 nm and ±17 nm for the 1-μm and 2-μm regions, respectively, and ±30 nm and ±47 nm for the OMEGA spectra.

Average uncertainty in the 1-μm region is ±30 nm and for the 2-μm region is ±47 nm (Table 5). The uncertainty values for the LCP components are smaller for the LCP-rich terrain compared to the HCP-rich terrain and vice versa, the uncertainty for the HCP components is smaller for the HCP-rich terrain compared to the LCP-rich terrain.

We compare the uncertainty observed in our Monte Carlo approach to the formal constraints for the OMEGA spectra. While the final band positions are within the expected range for terrestrial pyroxenes the constraints are at least an order of magnitude larger than the uncertainty parameter derived using the methodology in our analysis. In general, the formal constraints are larger for the HCP-rich terrain compared to the LCP-rich, which also has larger band depths.

5.2. *Sensitivity Test 2: Band strength and pyroxene mixtures*

The second sensitivity test investigates how the MGM performs for pyroxene mixtures of various compositions. Endmember MGM fits for the martian meteorite spectra, ALH84001 and MIL03346, used in the second sensitivity test are evaluated and compared to the fits of ALH84001 and Nakhla from Sunshine et al. (2004a). For both meteorite samples used in this study, the model suggests the presence of only one pyroxene phase. Consistent with their compositions, the fit of the orthopyroxenite AHL84001 requires only LCP absorptions (Fig. 10, solid line) and the high-calcium dominated nakhlite MIL03346 requires only HCP absorptions (Fig. 10, dashed line). Both spectra are also modeled with a M1 absorption at 1.2 μm, which is significantly stronger for the nakhlite compared to the orthopyroxenite. Sunshine et al. (2004a) modeled similar absorptions for ALH84001 and Nakhla and was able to resolve an additional M1 absorption near 0.92 μm for the nakhlite, which is predicted by crystal field theory (Burns, 1993). While our fit of MIL03346 does not obviously require an additional near 0.9 μm it is possible that the second 1 μm absorption is also present considering the uniquely strong M1 absorption near 1.2 μm.

We use these martian meteorites with additional pyroxene phases to define a robust relationship between modal abundance and component band strength. We calculate a normalized band strength ratio, LCP/(LCP + HCP), for the 1- and 2-μm regions. This ratio acts as a proxy for the predicted fraction of LCP in the mixture. This calculation is a different representation of the same type of data described by Sunshine and Pieters (1993), who investigate LCP/HCP band strength relationship versus relative %HCP for one enstatite–diopside mixture. The incorporation of a normalized band strength ratio allows for the known fraction of LCP in the mixture as well as the predicted fraction to range between zero and one. Thus, we can investigate a linear correlation between the known and predicted modal abundance rather than a higher order polynomial as shown in Sunshine and Pieters (1993) and Sunshine et al. (2004b).

The relationship between the known and the predicted fraction of LCP in the mixture in the 1- and 2-μm regions are plotted in Fig. 11. We compare the results for all iterations in the 1- and 2-μm regions to the results after removal of inappropriate

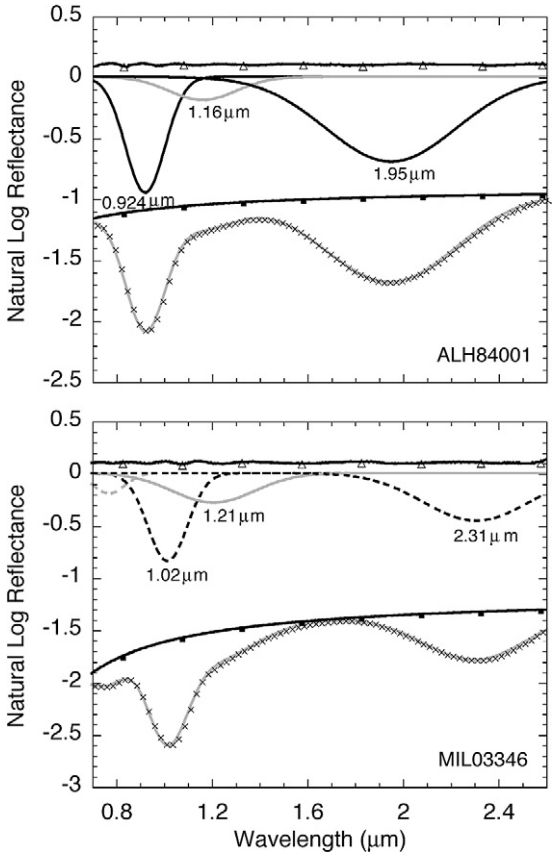

Fig. 10. Final MGM fits for the orthopyroxenite ALH84001 and the nakhlite MIL03346. The fit of ALH84001 requires only LCP absorptions (solid line absorption) while the fit of MIL03346 requires only HCP absorptions (dashed line absorption). Both spectra are also modeled with an additional absorption at ∼1.2 μm. The 1.2-μm absorption is stronger for the nakhlite compared to the orthopyroxenite. MGM deconvolved band positions are noted for each absorption.

fits. It is noteworthy that for all comparisons, results from the martian meteorite mixture (Mixture #6) behave similarly to all other mixture spectra. Normalized band strength ratios for all iterations show a scattered correlation between the known and predicted LCP fractions in the 1-μm region (Fig. 11A). Compared to these scattered results in the 1-μm region, results for the 2-μm region for all iterations indicate a near 1:1 correlation (Fig. 11B). The trends between the known and predicted mixtures when the inappropriate fits are removed are shown for the 1-μm region (Fig. 11C) and for the 2-μm region (Fig. 11D). In this scenario, which includes all satisfactory fits, the near 1:1 correlation holds for both the 1- and 2-μm regions. The trend in the 1-μm region is significantly better when inappropriate fits are removed. The trend in the 2-μm region is similar before and after removal of all inappropriate fits. We make this comparison before and after removal of unsuccessful iterations to demonstrate that the cause of failure as observed in individual fits can be attributed to poor results in the 1-μm region. This in turn suggests that the 2-μm region is a better region for determining relative band strength.

We also observe that the near 1:1 correlation between the predicted and known fraction after the removal of inappropriate fits is slightly offset from the 1:1 line such that it predicts

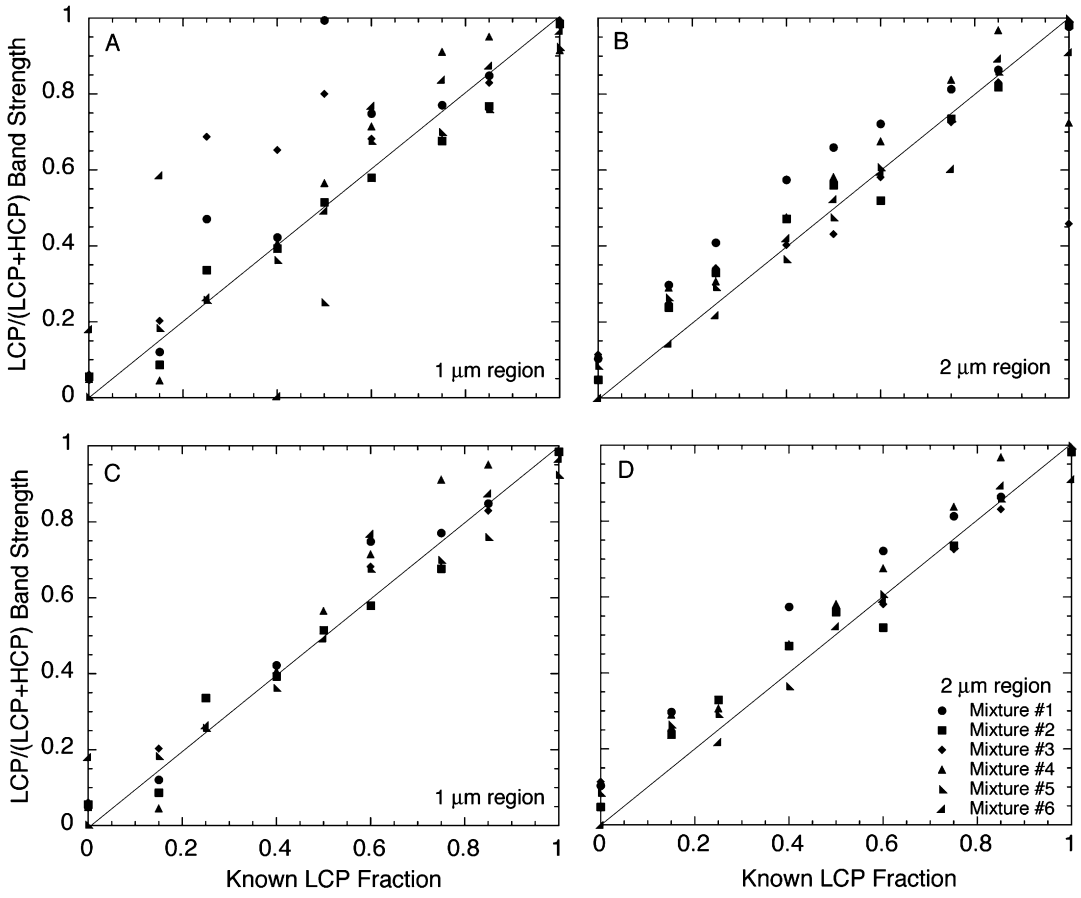

Fig. 11. Normalized band strength ratio, LCP/(LCP + HCP), in the 1-μm (A, C) and 2-μm (B, D) regions versus the relative known fraction of LCP in the mixture for each mixture series. The diagonal line represents the 1:1 trend. (A) and (B) record the results from all iterations, while (C) and (D) exclude fits that did not meet the described criteria. Comparison of (A) and (C) indicate that more fits failed in the 1-μm region, while the trend in the 2-μm region (B) and (D) is consistent throughout. The normalized band strength ratio can predict the relative fraction of LCP in a pyroxene mixture within ±10%.

an overabundance of LCP. The calculated bias for the correlation in the 2-μm region is about +4%. To investigate this shift more explicitly we calculate a normalized band strength ratio where the individual LCP and HCP band strengths are each normalized to their corresponding endmembers. This second normalization should mitigate inherent differences in the absolute band strength between LCP and HCP spectra. Comparison of this second normalization for the predicted LCP fractions to the initial predicted LCP fractions reveal a corrected trend that is shifted closer to the 1:1 line. The calculated bias for the 2-μm region after the second normalization is reduced to about +1%. However, in application of the MGM to remotely acquired datasets the endmembers are inherently unknown and this second normalization is impossible. Furthermore, differences in the twice-normalized data and initial normalization are less than the absolute differences for a given modal abundance of various compositions.

For practical use of the MGM where the procedure is independent of the endmember compositions, we evaluate uncertainties for the once normalized data. Uncertainty values on the predicted fractions of LCP are calculated as an RMS difference between the predicted LCP fraction and the expected value on the 1:1 line. The RMS value for the 1- and 2-μm regions is ∼8%. This uncertainty indicates that a normalized band strength derived from the MGM can conservatively predict the relative fractions of LCP and HCP to ±10% (1 STD). This error in relative abundance estimates is in agreement with that found in Sunshine et al. (1993) and presents a significant improvement in that a wider range of pyroxenes is investigated here.

The effect of adding olivine to Mixture #1 differed for the 1-μm region compared to the 2-μm region. The addition of up to 20% olivine did not significantly affect calculations of the pyroxene normalized band strength ratio in the 2-μm region. The difference between the normalized band strength ratios of the pure pyroxene mixture and the pyroxene and olivine mixtures was always less than 8%, which was the RMS determined for pure pyroxene mixtures of various compositions. However, determination of the LCP fraction for the 1-μm region within ±10% fell off with the addition of 10–15% olivine. Because the dominant spectral feature of olivine occurs at ∼1 μm, it is important to use the value of 10–15% olivine as the limit of the fraction of olivine that can be present without affecting the derivation of the modal pyroxene abundance. The consequence of the olivine addition on other band parameters, specifically the increased width of the 1.2-μm feature with increased olivine content was also noted, but not characterized in further detail in this analysis.

Table 6
Resulting band positions and strengths for the averaged OMEGA spectra selected from the Syrtis Major (SM) and Valles Marineris (VM) provinces

Spectral feature	SM Hesperian volcanics	Melas Chasma	VM valley floor	Noachian terrain north of SM	VM outflow channels	South of VM outflow channels
LCP 1 μm						
Center	0.891	0.885	0.882	0.896	0.900	0.901
Strength	0.140	0.136	0.172	0.131	0.138	0.110
HCP 1 μm						
Center	1.048	1.039	1.026	1.024	1.025	1.036
Strength	0.168	0.088	0.146	0.089	0.036	0.043
LCP 2 μm						
Center	1.903	1.860	1.802	1.862	1.842	1.860
Strength	0.093	0.096	0.156	0.143	0.172	0.137
HCP 2 μm						
Center	2.305	2.320	2.280	2.280	2.292	2.307
Strength	0.145	0.146	0.164	0.099	0.163	0.095
%LCP(±10%)[a]	39	40	49	59	51	58

Note. The band center is given in microns (μm) and the band strength in natural log reflectance.
[a] %LCP is the percent of LCP relative to HCP and is calculated from the normalized band strength ratio (LCP/(LCP + HCP)) in the 2-μm region.

5.3. Application of sensitivity tests

MGM solutions for the averaged pyroxene-rich OMEGA spectra indicate a two-pyroxene composition for all spectra. Based on relative band strengths the sampled spectra can be divided into two types of terrains, those relatively enriched in LCP (terrain around Valles Marineris and the ancient terrain north of Syrtis Major) and those relatively enriched in HCP (deposits within the Valles Marineris canyon system and the Syrtis Major volcanics). The highest modal abundance of LCP and the highest modal abundance of HCP occur for spectra in the Syrtis region (Table 6). The LCP-rich ancient Noachian terrain north of Syrtis yields a normalized band strength ratio indicative of 59 ± 10% LCP while the HCP-rich Syrtis volcanics indicate 39 ± 10% LCP.

The band positions of the averaged spectra plot within the range of terrestrial pyroxene band centers (Adams, 1974; Cloutis and Gaffey, 1991; Fig. 12, Table 6). The HCP components plot within the HCP field and the LCP components plot near the LCP field. Small differences are observed between the band positions of the LCP-rich terrains and the HCP-rich terrains. For HCP-rich terrains especially, the LCP band positions fall at shorter wavelengths in the 1-μm region compared to terrestrial pyroxenes. This trend was also observed for the HCP-rich terrain in the band center sensitivity test (Fig. 9). Also with respect to the HCP-rich terrains, the LCP band positions in the 2-μm region show a spread of ∼100 nm. For the LCP-rich and HCP-rich terrains, the 2-μm HCP band position remain clustered near the 2.3-μm starting position while the 1-μm HCP band position varies more significantly within the range of terrestrial pyroxenes.

Application of the uncertainty determined in the band center sensitivity test to the spatially averaged pyroxene-rich spectra reveals that small differences in band positions are within the calculated uncertainty. Thus, while we are confident in the two-pyroxene detection, direct correlations between endmember band position and specific pyroxene compositions are not made at this time. For comparisons of relative chemistries, additional spectra within each region would have to be included in the analysis.

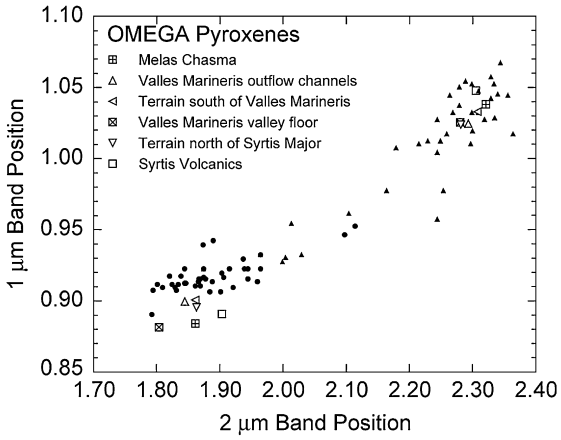

Fig. 12. MGM derived band positions for averaged OMEGA spectra of pyroxene-rich terrains. Deconvolution indicates a two-pyroxene composition for all spectra. While differences in band positions are observed between the various terrains, such variation is within the calculated uncertainties for OMEGA spectra (Fig. 9, Table 5). Band positions are plotted with the band positions for single-phase terrestrial pyroxenes as measured by Adams (1974) and Cloutis and Gaffey (1991). Orthopyroxenes are given by closed circles and clinopyroxenes by closed triangles.

6. Discussion

The sensitivity tests developed in this study address the strengths and limitations of the MGM that are essential to consider for application to remotely acquired data. We explore the sensitivity of the input parameters and ability of the MGM to find unique resultant band positions as well as the ability to predict the LCP fraction for a variety of calculated pyroxene mixtures. By testing the MGM with spectra that are representative of extraterrestrial pyroxenes, we calculate uncertainty parameters that describe the ability for the MGM to derive pyroxene composition and pyroxene modal abundance.

6.1. Deconvolution of pyroxene composition

Reasonable systematic variation for the input parameters in the 1- and 2-μm regions found multiple solutions for both laboratory (Fig. 8) and remotely acquired spectra (Fig. 9). To determine if the multiple solutions existed within a small enough range such that we could be confident in compositional differences, we explored trends in the resultant band positions as an average and standard deviation. All average band positions and uncertainties for the martian meteorites Zagami and Shergotty and OMEGA spectra plotted within the range of single-phase terrestrial pyroxenes. This result is encouraging and confirms that the MGM can be appropriately applied to remotely acquired spectra and retrieve reasonable results. This is especially

significant since the spectral contrast and signal to noise ratio for remotely acquired spectra are less favorable compared to laboratory spectra.

Highlighted in this sensitivity test are some important considerations for application of the MGM to remotely acquired spectra and for retrieval of unique band positions. Comparison between the starting parameters and resultant solutions for multiple iterations showed that the final band positions varied with the values of the starting parameters. This relationship between the starting and resultant parameters emphasizes that careful consideration and explicit rationale need to be given to determination of the starting parameters.

Resultant band positions for the OMEGA spectra revealed small variations that require further explanation. For the HCP-rich terrains especially, the 1-μm LCP feature exhibited band positions at shorter wavelengths compared to the terrestrial pyroxenes. A similar trend for the 1-μm LCP component was also observed in the work of Mustard et al. (1997) who applied the MGM to ISM pyroxene-rich spectra. We believe that this movement in band position may be attributed to the presence of the ferric absorption at ∼0.85 μm and the lack of a dominant LCP component in the HCP-rich terrain. Without a strong LCP feature in the 1-μm region, the 1-μm LCP absorption can become confused with and migrate toward the ferric component. An additional explanation for the lower than expected movement of band positions could be due to the presence of aluminum. (Cloutis et al., 1990).

The presence of multiple valid solutions offers an important uncertainty parameter on resultant band positions derived from the MGM complimentary to the formal output constraints. The uncertainty values are measured as a standard deviation from the results of the Monte Carlo approach and differ for the laboratory and remotely acquired spectra. The uncertainty is smaller for the SNC meteorites compared to the OMEGA spectra. This is expected because the band depth and spectral contrast are greater for the laboratory spectra compared to the remotely acquired data. The derived average uncertainty for the OMEGA band positions in the 1-μm (±30 nm) and 2-μm (±47 nm) region encompasses a significant portion of the range of appropriate pyroxene band positions. Nevertheless these calculated uncertainties are smaller by at least an order of magnitude compared to the formal output constraints. Thus, solutions from this sensitivity test suggest that resultant band positions derived from the MGM for OMEGA spectra produce reasonable values but cannot be absolutely correlated to pyroxene compositions without consideration of an appropriate uncertainty. With a reasonable sample size it could be possible to determine relative changes in composition using OMEGA data. MGM deconvolution of remotely acquired data with a higher signal-to-noise ratio and greater spectral contrast than OMEGA could yield band positions that would be appropriate to discern absolute and relative chemistries. This assessment is supported by results from the laboratory meteorite spectra that have higher spectral contrast and lower noise and absolute compositions can be assessed from derived band positions. Sunshine et al. (2004b) have used SpeX asteroid data to examine relative chemistries and there is significant potential to conduct similar analyses using CRISM (Compact Reconnaissance Imaging Spectrometer for Mars) data.

6.2. Deconvolution of modal abundance

We tested the performance of the MGM for mixtures of various compositions representative of extraterrestrial pyroxenes to examine the trends between the known and predicted modal abundances. The results of the martian meteorite mixture of the orthopyroxenite ALH84001 and the nakhlite MIL03346 behave similarly to the other mixture series, which further supports the assessment that the MGM is an appropriate analytical tool for extraterrestrial datasets.

Comparison of the results before and after the removal of inappropriate fits suggests that fits fail more easily in the 1-μm region rather than the 2-μm region. This failure can be attributed to the greater number of deconvolved and overlapping absorptions for the 1-μm feature compared to the 2-μm feature.

The MGM application to pyroxene mixtures with a range of compositions demonstrates a strong relationship between the normalized LCP/(LCP + HCP) band strength ratio and the known fraction of LCP in the mixture. The robust relationship in the 2-μm region and the 1-μm region when inappropriate fits are removed shows that without prior knowledge of pyroxene composition or absolute abundance it is possible to use a normalized band strength ratio and estimate the relative pyroxene abundance. Conservative uncertainty values for the modal abundance estimates are ±10%.

Even with the addition of at least 20% olivine determination of modal pyroxene abundances is robust using the normalized band strength ratio in the 2-μm region. The inconsistent results in the 1-μm region at 10–15% olivine are expected because of the prominent 1-μm feature of olivine. Thus, we use the 1-μm limit as the maximum amount of olivine. It is noteworthy that the band depth of olivine used in this analysis is equal in band depth to the LCP component. Thus, the 10–15% olivine content is a minimum amount that would affect MGM results for a pyroxene-dominated spectrum. For mineral components with absorption features at ∼1 μm with weaker band depths than the dominant pyroxene, the absolute abundances in the mixture could be greater than 10–15% without affecting the modeled solutions and derived pyroxene abundances.

These results indicate that the MGM is a particularly valuable analytical tool for investigation of remotely acquired spectra that exhibit the characteristic 1- and 2-μm pyroxene absorptions. It should be noted that not all pyroxene spectra exhibit typical 1- and 2-μm features. Such spectra have been explored in some detail (e.g., Adams, 1975; Cloutis and Gaffey, 1991; Schade et al., 2004) and represent compositions that lack iron in the M2 crystallographic site. Thus, these spectra do not exhibit the M2 absorption at 2 μm and the performance of the MGM on these types of atypical spectra is not considered in this analysis. Results in this study are complementary to previous work that also explored the systematics of standard (characterized by 1- and 2-μm absorption features) pyroxene spectra and suggested that resultant solutions were independent of grain size (Sunshine and Pieters, 1993). The mixture series analy-

sis developed in this paper indicates that MGM solutions are also independent of composition as long as M2 absorptions, rather than M1 absorptions, dominate the spectrum. For these reasons, it is appropriate and valuable that we apply the MGM to pyroxene-dominated OMEGA spectra for the surface of Mars and other extraterrestrial surfaces.

6.3. Deconvolution of OMEGA spectra

The distribution of pyroxene-rich terrains on Mars identified in this study using the MGM is consistent with results from previous work with respect to the derived modal pyroxene abundances. Modal abundance estimates used in this study are derived from a normalized band strength ratio (LCP/(LCP + HCP)), similar to Sunshine and Pieters (1993) who investigate an LCP/HCP band strength ratio. The ancient terrains north of Syrtis Major and those associated with the Valles Marineris outflow channels indicate a relative enrichment in low-calcium pyroxene while the younger deposits in Syrtis Major and Valles Marineris indicate local terrains enriched in high-calcium pyroxene (Bandfield, 2002; Hamilton et al., 2003; Mustard et al., 2005; Gendrin et al., 2006). This study builds on previous works by incorporating the MGM with all free parameters to the 1- and 2-μm absorption and by evaluating the results using uncertainty parameters derived in this analysis. The aforementioned pyroxene dichotomy of LCP enrichment in the ancient terrain and HCP enrichment in the Syrtis volcanic flows establishes several important questions about the nature and evolution of the mantle source regions. The dominance of the low-calcium pyroxene observed by OMEGA in ancient terrain may indicate that the martian mantle experienced more extensive melting early in its history. The compositional change to deposits that are relatively enriched in high-calcium pyroxene during the Hesperian epoch may be indicative of smaller extents of melt due to the monotonic cooling of the planet. Other explanations could be related to the depth of the melting or that the melt endured near-surface re-equilibration or assimilation on its traverse to the surface.

Refinement of pyroxene composition is valuable to determine subsurface evolution. However, while the resultant band positions deconvolved in this study are all reasonable values, they exist within the derived uncertainty. Thus, it is difficult to explicitly distinguish variations in compositions with this sample size at this time. Perhaps with a larger sample size with the current dataset, changes in relative composition could be examined. For remote datasets with lower noise and higher spectral contrast, it is also likely that relative and absolute changes in composition could be determined. Furthermore, results in this study showed that the uncertainty for the band positions of the laboratory spectra of Zagami and Shergotty were significantly smaller than those derived from OMEGA spectra (Table 5, Figs. 8, 9). It is possible to discern relative compositional changes for martian meteorite data. For example, using laboratory data, Sunshine et al. (1993) successfully compared relative compositional variations between Lithologies A and B of the Elephant Moraine A79001 martian meteorite.

Further investigation of the OMEGA data using the MGM may reveal important trends in the composition and modal abundance and provide the necessary refinement to understand the nature of melt extraction and course to the surface. We note that this study is unique in that the MGM is conducted with all free parameters. Many other MGM investigations have incorporated covariance parameters or fixed parameters for stronger encouragement of the MGM to obtain a reasonable result (Combe et al., 2004; Gendrin et al., 2006; Pinet et al., 2006). Perhaps with tighter restrictions, significant compositional trends can be resolved to provide further constraints on mantle evolution.

7. Conclusion

To understand the evolution of the surface and interior of planetary bodies it is essential to refine the spatial and spectral identifications of the mafic minerals. The Modified Gaussian Model (MGM) developed by Sunshine et al. (1990) is a valuable analytical tool to extract modal pyroxene abundance and compositional endmember estimates without the use of a spectral library. Complementary to the previous study of Sunshine and Pieters (1993), which showed that MGM solutions of pyroxene mixtures were independent of particle size, sensitivity tests developed in this analysis also indicate that the model is independent of endmember composition. A normalized band strength ratio of the low-calcium and high-calcium endmember pyroxene components can confidently be used to estimate modal abundance within ±10% (1 STD). This calculation is robust with the minimum addition of 10–15% olivine to the pyroxene mixture. Subsequent tests also indicate that a full application of the MGM (inclusive of the 1- and 2-μm absorptions) can be incorporated in studies using remotely acquired data and find reasonable solutions. Deconvolved band positions of OMEGA spectra for Mars exist within the range of terrestrial band positions and assessments of the normalized band strength ratios for a variety of pyroxene-rich terrains on the martian surface are consistent with previous analyses (Bandfield, 2002; Mustard et al., 2005; Gendrin et al., 2006). However, while different martian terrains exhibit small variations in band positions, these small differences lie within the calculated uncertainties of ±50 nm (1 STD) for MGM fits with all parameters free. Thus, estimates to refine absolute pyroxene compositions, which can be directly derived from band position, are not robust with our analysis of OMEGA data at this time. Further studies of OMEGA data could reveal relative compositional variations and further studies of remote measurements with greater spectra contrast and higher signal-to-noise (e.g., SpeX asteroid data and CRISM Mars data) could reveal more precise estimates on absolute compositions.

Acknowledgments

The authors thank the OMEGA–Mars Express team for outstanding support in reduction of data and to Rachel Klima and RELAB for providing laboratory spectra. We thank J. Sunshine and E. Cloutis whose comments and suggestions have helped

to significantly improve the manuscript. This work is funded by NASA's Rhode Island Space Grant Consortium, a grant from NASA Planetary Geology and Geophysics to J.F.M., and by the Marie Curie OIF fellowship #8579.

References

Adams, J.B., 1974. Visible and near-infrared diffuse reflectance: Spectra of pyroxenes as applied to remote sensing of solid objects in the Solar System. J. Geophys. Res. 79, 4829–4836.

Adams, J.B., 1975. Interpretation of visible and near-infrared diffuse reflectance spectra of pyroxenes and other rock-forming minerals. In: Karr, C. (Ed.), Infrared and Raman Spectroscopy of Lunar and Terrestrial Minerals. Academic Press, New York, pp. 91–116.

Bandfield, J.L., 2002. Global mineral distributions on Mars. J. Geophys. Res. 107 (E6), doi:10.1029/2001JE001510. 5042.

Bibring, J.-P., and 16 colleagues, 1989. Results from the ISM experiment. Nature 341, 591–593.

Bibring, J.-P., and 42 colleagues, 2004. OMEGA: Observatoire pour la Minéralogie, l'Eau, les Glaces et l'Activite. European Space Agency Spec. Publ. 1240, 37–49.

Bibring, J.-P., and 16 colleagues, 2005. Mars surface diversity as revealed by the OMEGA/Mars Express observations. Science 307, 1576–1581.

Bishop, J.L., Pieters, C.M., Hiroi, T., Mustard, J.F., 1998. Spectroscopic analysis of martian meteorite Allan Hills 84001 powder and applications for spectral identification of minerals and other soil components on Mars. Meteorit. Planet. Sci. 33, 699–707.

Burns, R.G., 1993. Mineralogical Applications of Crystal Field Theory, second ed. Cambridge Univ. Press, New York.

Cameron, M., Papike, J.J., 1980. Crystal chemistry of silicate pyroxenes. In: Prewitt, C.T. (Ed.), Reviews in Mineralogy 7: Pyroxenes. Mineralogical Society of America, Washington, DC, pp. 5–92.

Cloutis, E.A., 2002. Pyroxene reflectance spectra: Minor absorption bands and effects of elemental substitutions. J. Geophys. Res. 107, 6-1–6-12.

Cloutis, E.A., Gaffey, M.J., 1991. Pyroxene spectroscopy revisited: Spectral–compositional correlations and relationship to geothermometry. J. Geophys. Res. 96, 22809–22826.

Cloutis, E.A., Gaffey, M.J., Smith, D.G.W., Lambert, R.S.J., 1990. Metal silicate mixtures: Spectral properties and applications to asteroid taxonomy. J. Geophys. Res. 95 (B6), 8323–8338.

Combe, J.-Ph., Le Mouelic, S., Sotin, C., Bibring, J.-P., and The OMEGA Team, 2004. Mineralogical Study by MGM Analysis of OMEGA/Mars Express Hyperspectral Data. Runion des Sciences de la Terre, Strasbourg, France.

Dyar, M.D., Treiman, A.H., Pieters, C.M., Hiroi, T., Lane, M.D., O'Connor, V., 2005. MIL03346, the most oxidized martian meteorite: A first look at spectroscopy, petrography, and mineral chemistry. J. Geophys. Res. 110, doi:10.1029/2005JE002426. E09005.

Elkins-Tanton, L.T., Parmentier, E.M., Hess, P.C., 2003. Magma ocean fractional crystallization and cumulate overturn in terrestrial planets: Implications for Mars. Meteorit. Planet. Sci. 38, 1753–1771.

Gendrin, A., and 10 colleagues, 2006. Strong pyroxene absorption bands on Mars identified by OMEGA: Geological counterpart. Lunar Planet. Sci. XXXVII. Abstract 1858.

Hamilton, V.E., Christensen, P.R., McSween, H.Y., Bandfield, J.L., 2003. Searching for the source regions for the martian meteorites using MGS TES: Integrating martian meteorites into the global distribution of igneous materials on Mars. Meteorit. Planet. Sci. 38, 871–885.

Hapke, B., 1981. Bidirectional reflectance spectroscopy. 1. Theory. J. Geophys. Res. 86, 3039–3054.

Hapke, B., 1986. Bidirectional reflectance spectroscopy. 4. The extinction coefficient and the opposition effect. Icarus 67, 264–287.

Hess, P.C., Parmentier, E.M., 2001. Implications of magma ocean cumulate overturn for Mars. Proc. Lunar Planet. Sci. XXXII. Abstract 1319.

Hiroi, T., Sasaki, S., 2001. Importance of space weathering simulation products in compositional modeling of asteroids: 349 Dembowska and 446 Asternitas as examples. Meteorit. Planet. Sci. 36, 1587–1596.

Klima, R.K., Pieters, C.M., Dyar, M.D., 2005. Pyroxene spectroscopy: Effects of major element composition on near, mid, and far-infrared spectra. Lunar Planet. Sci. XXXVI. Abstract 1462.

Longhi, J., Knittle, E., Holloway, J.R., Wänke, H., 1992. The bulk composition, mineralogy and internal structure of Mars. In: Kieffer, H., Jakosky, B., Snyder, C., Matthews, M. (Eds.), Mars. Univ. of Arizona Press, Tuscon, pp. 184–208.

McSween, H.Y., 1994. What we have learned about Mars from SNC meteorites. Meteoritics 29, 757–779.

Mittlefehldt, D.W., 1994. ALH84001, a cumulate orthopyroxenite member of the martian meteorite clan. Meteoritics 29, 214–221.

Mustard, J.F., Pieters, C.M., 1987. Quantitative abundance estimates from bidirectional reflectance measurements. J. Geophys. Res. 92, 617–626.

Mustard, J.F., Pieters, C.M., 1989. Photometric phase functions of common geologic minerals and applications to quantitative analysis of mineral mixture reflectance spectra. J. Geophys. Res. 94, 13619–13634.

Mustard, J.F., Sunshine, J.M., 1995. Seeing through the dust: Martian crustal heterogeneity and links to the SNC meteorites. Science 267, 1623–1626.

Mustard, J.F., Murchie, S., Erard, S., Sunshine, J.M., 1997. In situ compositions of martian volcanics: Implications for the mantle. J. Geophys. Res. 102, 25605–25615.

Mustard, J.F., Poulet, F., Gendrin, A., Bibring, J.-P., Yangevin, Y., Gondet, B., Mangold, N., Bellucci, G., Altieri, F., 2005. Olivine and pyroxene diversity in the crust of Mars. Science 307, 1594–1597.

Pieters, C.M., 1983. Strength of mineral absorption features in the transmitted component of near-infrared reflected light: First results from RELAB. J. Geophys. Res. 88, 9534–9544.

Pieters, C.M., Hiroi, T., 2004. RELAB (Reflectance Experiment Laboratory): A NASA multiuser spectroscopy facility. Lunar Planet. Sci. XXXV. Abstract 1720.

Pinet, P.C., and 12 colleagues, 2006. Mantle rock surface mineralogy mapping in arid environment from imaging spectroscopy: The case of the Masqad peridotitic massif in Oman and implications for the spectroscopic study of exposed mafic units on Mars. Lunar Planet. Sci. XXXVII. Abstract 1346.

Schade, U., Wäsch, R., 1999. Near-infrared reflectance spectra from bulk samples of the two SNC meteorites Zagami and Nakhla. Meteorit. Planet. Sci. 34, 417–424.

Schade, U., Wäsch, R., Moroz, L., 2004. Near-infrared reflectance spectroscopy of Ca-rich clinopyroxenes and prospects for remote spectral characterization of planetary surfaces. Icarus 168, 80–92.

Stopler, E.M., McSween, H.Y., 1979. Petrology and origin of the shergottite meteorites. Geochim. Cosmochim. Acta 43, 1475–1498.

Sunshine, J.M., Pieters, C.M., 1993. Estimating modal abundances from the spectra of natural and laboratory pyroxene mixtures using the Modified Gaussian Model. J. Geophys. Res. 98, 9075–9087.

Sunshine, J.M., Pieters, C.M., Pratt, S., 1990. Deconvolution of mineral absorption bands: An improved approach. J. Geophys. Res. 95, 6955–6966.

Sunshine, J.M., McFadden, L.-A., Pieters, C.M., 1993. Reflectance spectra of the Elephant Moraine A79001 meteorite: Implications for remote sensing of planetary bodies. Icarus 105, 79–91.

Sunshine, J.M., Pieters, C.M., Pratt, S.F., McNaron-Brown, K.S., 1999. Absorption band modeling in reflectance spectra: Availability of the Modified Gaussian Model. Lunar Planet. Sci. XXX. Abstract 1306.

Sunshine, J.M., Bishop, J., Dyar, D., Hiroi, T., Klima, R., Pieters, C.M., 2004a. Near-infrared spectra of martian pyroxene separates: First results from Mars Spectroscopy Consortium. Lunar Planet. Sci. XXXV. Abstract 1636.

Sunshine, J.M., Bus, S.J., McCoy, T.J., Burbine, T.H., Corrigan, C.M., Binzel, R.P., 2004b. High-calcium pyroxene as an indicator of igneous differentiation in asteroids and meteorites. Meteorit. Planet. Sci. 39, 1343–1357.

Tarantola, A., Valette, B., 1982. Generalized nonlinear inverse problems solved using the least squares criterion. Rev. Geophys. Space Phys. 20, 219–232.